

---

**NINA**

**The 4 GeV Electron Synchrotron of  
The National Institute for Research  
in Nuclear Science**

---

**Daresbury Nuclear Physics Laboratory**

Daresbury, Nr. Warrington, Lancashire

---

**N I N A**

**The 4 GeV Electron Synchrotron of  
The National Institute for Research  
in Nuclear Science**



# The 4 GeV Electron Synchrotron of the National Institute for Research in Nuclear Science

## 1. INTRODUCTION.

The Daresbury Nuclear Physics Laboratory was set up by the Governing Board of the National Institute for Research in Nuclear Science on July 18th, 1962. Its present programme is to build a 4 GeV electron synchrotron (NINA) and the laboratory to house it. A great deal of preliminary planning had been done before the laboratory was started by a working party under the chairmanship of T. G. Pickavance, and under an extra-mural contract with J. M. Cassels at Liverpool University. Since July 1962 a site has been found for the laboratory, the basic physical design of the machine has been settled, and the detailed design of the buildings has been completed. Contracts for the buildings and for most of the major components of the synchrotron have already been let. In this report the present status of the laboratory and the synchrotron is outlined.

It was assumed from the first in designing the synchrotron that it should be of the strong-focusing kind, where the electron beam circulating in the accelerator is confined to a small region by very strong magnetic forces. The virtues of such an electron accelerator have since been demonstrated in a very striking way by the successful operation in September 1962 of the joint Harvard-MIT electron synchrotron designed on these principles, and the DESY accelerator at Hamburg in February 1964. A similar machine is under construction at Yerevan in Soviet Armenia.

The electrons in NINA will be steered in a circle of 70.2 metres diameter by 40 magnet units, each unit of length 3.3 metres (see Fig. 1). The gaps between these magnets will be alternately 1 and 3.5 metres. These very long field-free straight sections are a feature of the machine which should make it particularly accessible for experiments. Although the design energy of the machine is 4 GeV, the magnet will be capable of energies in excess of this, perhaps as much as 5.3 GeV.

The large diameter of the machine has been chosen so that radiation losses from the electrons are reduced, and to accommodate the large number of long straight sections in the accelerator.

The acceleration of the electrons will take place at five radio frequency stations around the machine. Again, this number has been made small so that as many straight sections as possible will be available for experiments.

The electrons will be injected into NINA from a 40 MeV linear accelerator and it is hoped that currents in excess of 1  $\mu$ A and perhaps as large as 10  $\mu$ A will be accelerated.

## 2. LABORATORY BUILDINGS.

The 50-acre site at Daresbury, Cheshire, acquired for the Daresbury Laboratory will accommodate the 4 GeV synchrotron and its associated buildings, and ensures a reasonable area for future expansion. The initial area of development will be about 15 acres. The area of the buildings now designed and approved is approximately 2.76 acres. The U.K. Atomic Energy Authority's Engineering Group has been responsible for the detailed design of the buildings.

The buildings have been laid out to provide the most convenient arrangement for doing experiments with NINA, and to ensure adequate space for any subsequent development. The contours of the ground have been carefully considered in order to reduce the amount of excavation and levelling to a minimum. Fig. 2 is a scale plan of the 50-acre site showing the area of development, and a photograph of a model of the site (Fig. 3) shows the layout of the buildings.

The development of the estate side of the site has been carried out in close co-operation with the

Planning Department of the Cheshire County Council who have given us every assistance to make the site a pleasant area which will conform to the existing rural pattern of the neighbourhood.

It is convenient to divide the buildings into four main groups:—

- (a) Accelerator Buildings.
- (b) Services Buildings for the Accelerator.
- (c) Research Services Buildings.
- (d) Laboratory and Office Building.

#### **(a) Accelerator Buildings.**

The magnet design has determined the size, shape, and details of the Magnet Ring Building and the Injector Building.

A cross-section of the Magnet Ring Building is shown in Fig. 4. Its main feature is the independent magnet supports, i.e. independent of the Magnet Ring Building. These are tied together by a reinforced concrete cap ring, 2 ft × 3 ft in section and integral with the 60 concrete piers which rest on the sandstone rock at a depth of at least 24 ft. The magnet units sit on 40 supporting steel bed-plates, and these in turn are attached to the tops of the reinforced concrete magnet support columns. Movements in the Ring Building or the surrounding buildings should not in any way be transmitted to the magnet foundations.

Services to the magnet energising coils, radio-frequency cavities, vacuum pumps, etc., are carried in the lower part of the Ring Building and are fed where necessary to the area overhead.

Temperature control of the whole area is maintained to  $\pm 1^\circ\text{C}$  in order to maintain stability of the complex equipment housed in the Ring Building and of the foundations themselves.

In considering the survey requirements for the positioning of the magnet, it was obvious that if the whole central area were roofed in we should simplify the survey and gain the large space required for ancillary equipment for the accelerator. This resulted in the so-called Inner Hall and two C shaped areas flanking it. These are used to house electrical equipment such as the magnet power supply, radio frequency equipment, etc. The Inner Hall is at right angles to the Electron Hall and this arrangement makes it easy to carry out experiments on the outer and inner sides of the magnet ring. Equipment and shielding blocks are readily handled by two overhead cranes. The Inner Hall is 200 ft long and 95 ft wide and has a 15-ton crane with a hook height of 22 ft. The Electron Hall is 200 ft long and 110 ft wide and has a 25-ton crane with a hook height of 29 ft.

Provision is made for the supply of AC and DC power, demineralised cooling water and other services to both halls.

#### **(b) Services Buildings for the Accelerator.**

With one exception this group follows the normal run of such buildings, and consists of a high voltage out-door compound for incoming 33 kV supply, 11 kV supply switchroom, generator building, and boiler house. The exception is the water cooling supply which is taken from the Bridgewater Canal and after passing through heat exchangers is returned to the canal at a point about 1.5 miles away.

The electricity supply authority has arranged for 4,000 kVA to be available by late 1964. By 1967, 10,000 kVA will be available and the final supply of 15,000 kVA shortly afterwards. When the accelerator starts, up to 4 MW of DC power from generators or rectifiers will be available for experimental purposes. The power consumption of NINA alone is 1.9 MW.

#### **(c) Research Services Buildings.**

This group of buildings is associated with the research carried out in the Laboratory. The Control and Counting Room is a single unit 30 ft wide × 100 ft long and has a false floor 18 in deep, suitable for control and other cabling. Adequate tunnels carry services to and from the Magnet Ring Building, the Inner Hall and Electron Hall.

The main feature of the group is a frame building 60 ft wide and 180 ft long served, over its full length, by a 10-ton crane with a hook height of 22 ft. This building houses the Stores, Workshop and Ancillary Laboratory. This last has direct access to the Electron Hall, and will be used for the assembly and testing of heavy experimental equipment.

A small meal room and other facilities are available for staff working extended hours or shift work on the synchrotron.

#### (d) Laboratory and Office Building.

The purpose of this building is to provide suitable accommodation for the permanent staff and groups planning experiments on the synchrotron.

There are six laboratories 24 ft × 36 ft, some of which are directly accessible from outside the building. In this way visiting groups can use trailer units for housing electrical and other equipment required for experiments on the synchrotron. Adequate office accommodation is provided adjacent to these laboratories.

Other facilities include a Drawing Office, Photographic Laboratory, Electronic Laboratory and Machine Development Laboratory. A good sized Library and Common Room are also provided. Experience in other laboratories has shown that considerable economies may be made by keeping office accommodation down to a 12 ft module. The majority of offices are therefore 12 ft wide × 12 ft deep. The first floor is arranged so that the accommodation may be used for either small laboratories or offices, and adequate provision is made for administrative purposes, telephone facilities and other common requirements.

### 3. MAGNET.

#### (a) Basic Parameters.

The over-all size of the electron synchrotron is determined by the radius of the magnet sectors and the lengths of the straight sections between the sectors. The magnetic radius is fixed by the design energy of 4 GeV and the chosen value of the magnetic field corresponding to this energy. This field must be rather small, partly to avoid any approach to saturation but mainly to reduce the energy loss due to synchrotron radiation. This loss must be made good by the RF power supply and sets a limit to the beam current at full energy. The field at 4 GeV is conservatively chosen as 6.43 kG, and the resulting magnetic radius is 20.77 m. The magnet power supply will excite the magnet to 9 kG, so that a small current of electrons will be obtainable at energies up to 5.3 GeV.

The arrangement of the magnets follows the pattern  $\overline{F}\overline{O}D\overline{O}$  where F and D represent horizontally focusing and defocusing magnets and  $\overline{O}$ , O represent straight sections of different lengths (see Fig. 5). This arrangement was chosen in preference to the alternative FOFDOD because the required field gradient in the magnets is smaller by almost a factor of two. Also this arrangement avoids the awkward junction between magnets of different types in the FOFDOD arrangement.

Considerable thought has been given to the best way of providing long straight sections to give access to the circulating beam. A super-period structure with four long straights arranged symmetrically around the ring was examined in detail. Matching conditions which enabled this to be done without much increase in the amplitude of betatron oscillations or momentum compaction were worked out. This involved the use of four types of magnet. Finally it was decided to make a simple machine in which the straight sections were alternately 3.5 m and 1 m in length. Although this leads to a machine 15% larger than that with super-periods, the resulting simplicity of design seemed most desirable, and has the added advantage that many more long straight sections are then available.

The choice of Q, the number of betatron periods around the machine, is an important one. As a rough approximation, the mean value of the momentum compaction  $(\Delta r/r)/(\Delta p/p)$  is proportional to  $1/Q^2$ , and the sensitivity of the machine to magnet errors is proportional to  $n/Q$ , where n is the field index. The minimum value of the betatron oscillation amplitude occurs near  $Q = \frac{1}{2} N$  where N is the number of magnet periods around the ring. The value of N depends on the lengths of the individual magnets. Although shorter magnets imply a higher Q-value, the straight sections are correspondingly shorter and the field gradient in the magnets greater. The compromise chosen has  $N=20$  and  $Q=5.25$  which leads to magnets 3.26 m. long, with a field gradient of 2.2% per cm., and a momentum compaction factor of 0.0453. The n-value is 47.17 for the D magnets and -46.17 for the F magnets, the difference ensuring equal Q-values vertically and horizontally. The distance between the stop lines enclosing the working region in the  $(n_D, n_F)$  plane is 5% of  $n_D$  or  $n_F$ .

The aperture of the magnet was decided on the basis of estimated effects of magnet mis-alignment and field errors, the emittance and energy spread of the beam from the injector, and the synchrotron oscillations of the injected beam. The F and D magnets have different ratios of horizontal and vertical apertures accommodating the varying cross-section of the beam, the maximum being  $\pm 6.5$  cm horizontally and  $\pm 3.7$  cm vertically.

### (b) Design of the Magnet.

The magnet will be excited with 50 cycle alternating current together with direct current sufficient to make the minimum current close to zero. At all chosen amplitudes of excitation the field at injection will have the same time derivative so that the minimum field is positive at full amplitude and may be slightly negative at sufficiently small amplitudes when the machine is operating at reduced energies.

The choice of material for the magnet yoke is governed by its properties at the injection field of 64.3 G. The permeability of the material must be high at this field and the coercive force must be small. The most suitable steel is hot-rolled transformer steel and the magnet is assembled from die-cut laminations of this material 0.0185 ins thick. The laminations are glued together to form blocks 12.4 inches in thickness and each sector consists of nine such blocks, together with two specially shaped end blocks, mounted on a baseplate along an arc of a circle. There are 40 such units, 20 radially focusing and 20 radially de-focusing.

The exciting coils are wound with stranded conductor of rectangular section and cooled by tubes embedded in the resinous insulation. There are four pancake coils per magnet, the total number of turns being 40 for the D magnet and 32 for the F magnet. The ratio of turns is the same as that of the pole gaps on the orbit, i.e. 3.0 ins and 2.4 ins, and all magnets are excited in series.

The pole contour is basically a hyperbola modified at the sides, where it joins the vertical faces of the yoke, to provide the maximum extent of uniform field gradient (Fig. 6). At the same time excessive saturation at the edges must be avoided. The modification has been calculated using a method of conformal transformation in which the pole contour, considered as one of a set of equipotentials, is transformed on to a plane in which the equipotentials have a linear form. The constants of the transformation determine the plateau width of the field gradient whilst the choice of equipotential governs the maximum field on the contour, the width of the pole root and the co-ordinates of the contour in the physical plane.

At the ends of the magnets there occur two undesirable effects. One is the eddy current produced by the lines of force curving into the laminations; the other is the variation of magnetic length with radius due to the change in fringing field along the edge of the wedge-shaped gap. Both these effects can be practically eliminated by suitable shaping of the ends. In a two dimensional approximation the magnet gap should increase according to an exponential curve whose constants depend on the value of the gap well away from the end. Using this approximation a trial end block has been manufactured and corrections to the shape made on the basis of magnetic measurements.

At low fields, near injection, corrections are necessary for the effects of remanence and reduced permeability. These corrections are provided by pole-face windings designed to give dipole, quadrupole and sextupole components and continuously energised by direct current.

## 4. MAGNET POWER SUPPLY.

The 40 guide field magnets are excited with a fully biased waveform,

$$I(t) = I_{DC} - I_{AC} \sin \omega_A t$$

in which the unidirectional and sinusoidally varying current components are supplied by two separate power sources.

To avoid drawing a large reactive power from the AC current source it is necessary to use a circuit which is resonant at the operating frequency, and which in addition provides a path for the circulating DC bias current. It is desirable also that the direct current source should conduct a minimum of the AC circulating current, and that it should be located at, or near, the system earth potential.

These requirements are satisfied by the circuit shown in Fig. 7, in which the magnet inductance ( $L_m$ ) forms a resonant circuit with a capacitor ( $C_m$ ) and the DC by-pass choke inductance ( $L_{cb}$ ) forms a resonant circuit with capacitor ( $C_{cb}$ ). This arrangement was used for testing the two 40-inch model magnets, with the F and D sectors temporarily equipped with back leg windings for acting alternately as magnet or choke.

This simple circuit is not suitable, however, for the complete network since in order to obtain uniformity of field intensity it is necessary to provide a series connection of all magnet windings. This, together with the servo-system current control of the AC and DC power sources, would ensure equal magnet currents (neglecting leakage) and precision control of the set excitation level. Hence a direct series connection of the 20 F and 20 D magnets would require an excessively high circuit voltage

for the AC current component (approximately 140 kV) which is impractical for winding insulation reasons, leakage current amplitudes and power sources.

Similarly, a parallel connection of F and D magnet series pairs is not possible because of the difficulty of accurate current control in the parallel networks.

The method of connection used for the NINA magnet supply (see Fig. 8) is based on the system originally used at Princeton, and employs a resonant network in which the magnets are connected in a number of series groups, together with associated resonant capacitors; each group of magnet capacitors is connected in parallel with a winding of the energy storage choke and a choke resonant capacitor. One of the energy storage choke secondary windings is split into two identical halves for the insertion of the DC bias-current power source, and the network is earthed at this point.

In this circuit, if leakage is neglected, the magnet currents are identical. The voltage around the ring is not cumulative, as would be the case for a simple series connection, because at the resonant frequency under symmetrical network conditions, the voltage across each magnet/capacitor group is zero. For the earth position shown, the centre point of each choke secondary, capacitor and magnet group is at earth potential under symmetrical conditions and normally, therefore, the maximum voltage to earth at any point in the ring circuit cannot exceed half the group voltage.

The choice of the number of series-connected magnets per group is dependent on considerations of circuit voltage and choke design complexity. A practical choice, consistent with the requirements of circuit symmetry, would be either one or two series pairs of F and D magnets per group. We have chosen the latter, giving the 10 port network shown, with a basic circuit voltage of 14 kV rms (7 kV to earth).

The magnet excitation current, which is independent of the number of series magnet groups, is 681 amps DC and 481 amps (rms) AC, for a peak gap field intensity of 9,000 gauss.

The AC power is fed to the network via the energy storage choke which is equipped with primary windings for this purpose. Each secondary has an associated primary to ensure symmetrical power input and act as an equalising winding.

During resonant working the total network stored energy is constant, neglecting losses, and the magnet stored energy is transferred to the choke and back again once per cycle, with the capacitors storing a portion of this peak energy.

Whereas the value of the magnet resonant capacitor ( $C_m$ ) is fixed by the magnet inductance, the ratio of the choke inductance ( $L_{ch}$ ) to magnet inductance ( $L_m$ ), and hence the value of the choke resonant capacitor ( $C_{ch}$ ), is determined principally by the relative costs of choke and energy storage capacitor. A study has shown the economic optimum to lie in the region of  $L_{ch} = 2-3 L_m$ , so the ratio of  $L_{ch} = 2 L_m$  has been chosen. Since the AC voltages across each choke secondary and magnet group are identical in amplitude (but reversed in phase) and the DC bias-current is common to both, the resulting choke secondary current is:—

$$I_{ch}(t) = I_{DC} + \frac{1}{2} I_{AC} \sin \omega_A t$$

i.e. having a DC component of 681 amps and an AC of 241 amps (rms).

It is well known that capacitors using oil impregnants have a temperature coefficient of capacitance of the same magnitude but opposite sign to those using chlorinate impregnants. Hence a combination of both impregnant types in each of the capacitor bank sections will result in a network resonant frequency that is virtually independent of capacitor dielectric temperature changes (better than 0.01% per °C for a working dielectric temperature rise of 35°C).

It will be noted also that the resonant capacitor groups accept a constant charge from the DC bias power supply, in addition to the AC charge. This distributed charge is proportional to the DC voltage drop across the choke secondary windings and is negligible compared with the AC rating, except in the case of the magnet resonant capacitor at the DC connection point. This is subjected to nearly the full DC bias source voltage.

Under symmetrical conditions the network is seen as a purely resistive load by the AC power source. Because of this and the high circuit Q of approximately 100, the AC power supply required is less than 1,000 kW. Another virtue of the high Q value is that it reduces transient disturbances in the magnet network (except effects due to excitation of the network leakage capacitance) and assists stability in the accurate control of magnet current.

Due to slight saturation of the guide magnets at the peak 9,000 gauss excitation level the AC current



component departs from a pure sine wave. However, this departure is small, and does not produce any harmonic loading in the AC power source.

The DC bias current will be provided by a poly-phase rectifier set capable of 0—100% voltage control, incorporating a filter network to attenuate the inherent DC commutation ripple at the output terminals. It is important to limit this ripple amplitude since the DC is connected at a single point in the resonant magnet network, and hence the distributed capacitive leakage current of the network could cause differences in magnet current amplitudes.

Direct AC excitation of the magnet network from the public supply is impracticable because of the random variation in both "mains" frequency and voltage.

The network will therefore be excited by pulse excitation from a static device. The alternative of an alternator with speed controlled drive was rejected on the grounds of inflexibility.

The pulse power supply effectively isolates the resonant magnet network from the "mains" and supplies the network cyclic loss in the form of an impulse. This energy impulse (less than 2% of the peak magnet energy) is applied during the descending portion of the magnet current waveform, and the disturbance introduced is completely attenuated before the next particle accelerating period (rising portion of the magnet current waveform).

The pulse power supply operates by charging a capacitor from a controlled rectifier source through a filter choke. This capacitor is then discharged through a triggered valve into the energy storage choke primary via a pulse limiting choke.

The pulse power supply is designed to provide a pulse duration that is short compared with the accelerator period ( $2\pi/\omega_A$ ), and uses a charging circuit that causes minimum fluctuation of the "mains" input current. It is triggered by a signal fed back from the magnet network, and if the pulse occurs symmetrically about the zero point in the choke secondary AC current waveform no "forced frequency" excitation will occur. A limited adjustment of the accelerator frequency is possible by changing the phase of the pulse valve firing point with respect to the choke AC current zero, at the expense of an increased pulse current amplitude.

A secondary, but important effect, of the impulse is to excite the leakage capacitance of the network so that, depending on its nodal point, it acts as a transmission line and causes disturbance to the magnet current. These effects can be suppressed by changing the nodal frequency by suitable multiple impedance earthing.

The magnet current amplitude is held accurately constant by servo control loops in the DC and AC current sources. These servo loops control independently the set AC and DC current levels to 1 part in 10,000 and hence control the field time derivative at the injection field of 64 gauss to within 2%. In addition, this field time derivative can be sampled, and an error signal used to modify the reference to both the AC and DC servo loops over a small range. Fast acting voltage controls are superimposed on the main loop to suppress "mains" disturbance effects and a further control acts on the stepless variable rectifier transformer to maintain minimum rectifier grid control angles in steady state operation.

Many of the refinements of control and the detailed understanding of the magnet resonant network behaviour have been greatly assisted by the study of performance using a 1/10th scale model of the complete network.

## 5. RADIO-FREQUENCY ACCELERATION SYSTEM.

The RF System is designed to accelerate  $1.2 \times 10^{12}$  electrons per pulse to 4 GeV at a repetition rate of 50 pulses per second. This is a very large current (10  $\mu$ A mean) and it may be difficult to trap such a beam and keep it stable in phase during acceleration. However, from theoretical studies so far, it appears that, given sufficient versatile control of RF frequency, phase and amplitude, it should be possible. Such a beam will be considerably larger than that planned at other synchrotrons.

The electron beam is accelerated at five stations, uniformly distributed around the machine orbit in long straight sections, and arranged so as not to fall in the experimental area or in the inflector straight. They are offset from the centres of the straight sections so that survey lines are not obstructed, and maximum space is left for experimental and other facilities. Each accelerating station consists of a 3-cell resonant cavity, RF power being fed into the centre section from waveguide, the two other sections being coupled to it by central holes. The unit is operated in  $\pi$ -mode, the sections being  $\lambda/2$  in

length. The acceleration frequency is 407.88 Mc/s per second, this being one seventh of the injector frequency and 300 times the orbital frequency. The radio-frequency is locked in phase to the injector.

The voltage and power requirements are functions of time. During the acceleration cycle the energy gain per turn must make up the radiation loss which increases as the fourth power of the energy, and provide a net energy gain proportional to the rate of rise of the magnetic field. The cavity voltage is obtained from the sum of these two requirements, after allowing for the chosen stable phase angle. This phase angle will vary from a low value at injection for good trapping, to a high value at the end of the cycle to reduce the peak power requirement.

The RF power required is the sum of two components; the resistive losses in the cavities, proportional to the square of the cavity voltage, and the power transferred to the beam. To obtain the total power required from the transmitter we must add about 10% for waveguide loss, and a further 13% for transmission loss in the isolator. This gives a trapezoidal curve, rising from 60 kW to 480 kW during the acceleration period. The over-all mean power output is 150 kW.

The mean power dissipation in the cavities is not large and presents no serious problems. The cavity voltage is about the same as in other machines, and hence should cause no difficulty, though extreme cleanliness (e.g. from pump oil) must be maintained. The input window, however, may be more highly stressed than in previous synchrotrons because of the high beam loading. Because this is reactive as well as resistive, we have elaborate control mechanisms monitoring and controlling the RF voltage and phase. Cavity tuning itself will have to be checked between acceleration cycles.

The cavities are of copper, and the input vacuum window is of high purity alumina.

Each cavity is at the end of a short stub arm of aluminium waveguide of internal cross-section  $21'' \times 10.5''$  which is joined to a closed waveguide ring by a tee-junction. This waveguide ring is resonant, there being a whole number of wavelengths between each cavity tee-junction. The ring is concentric with the synchrotron magnet and is situated in the services tunnel. This coupling system gives widest tolerances on cavity tuning and smallest sensitivity to fluctuation on beam loading. The tee-junction coupling hole, the length of the stub arm, and the cavity coupling hole have been carefully chosen to achieve this. Midway between two of the cavities is a sixth tee-junction at which the power is fed into the ring system from the transmitter. It is designed to present a match to the transmitter under the highest power condition. Owing to the varying effective impedance presented by the beam (due to the current being constant as the voltage varies) this matched condition cannot be maintained at all power levels.

To safeguard the transmitter against the effects of this varying load, as well as against accidental mismatch, the power is fed to the input tee-junction through an isolator. This is a modified Raytheon IUH-11 ferrite resonance isolator designed for our frequency and power ratings.

The transmitter and control cubicles are situated in the South end of the Inner Hall, the power being fed down a short waveguide run to the input tee-junction. The output power (480 kW peak 150 kW mean) is obtained from an RCA 2054 super power triode working at 12 kV plate voltage with an over-all average efficiency of 30%. This is driven by an RCA 2041 tetrode operating at the same plate voltage and giving a peak output of 40 kW. It requires a peak drive of 400 W.

A pre-driver unit amplifies the output of a crystal controlled master oscillator to the required level and also supplies synchronising signals to the injector and elsewhere if required. The master oscillator is capable of rapid frequency modulation to allow tuning out of the reactive component of the beam loading. A phase modulation stage will be incorporated also, to assist in trapping the beam initially.

The circuits or "cavities" for the RCA tubes are being obtained from RCA. Gridded tubes were preferred to klystrons because of the complications introduced by the higher beam voltage of the klystrons and the difficulties of designing and manufacturing the modulating anode control circuit. The RCA tubes require good "crowbar" circuits on the plate and screen supplies.

A further cubicle in the Inner Hall houses the RF controls. Each cavity must be kept on tune on a long term basis. This will be done by automatic tuners, controlled by a phase detector which samples the cavity field and compares it with the input. Owing to the effect of beam loading, this will have to be done between acceleration cycles during a small "tuning pulse" of RF. The conditions at the input tee-junction will be monitored by directional couplers in the feed line, and the load will be made to look resistive by adjusting the RF frequency. It is planned to use "beam control" with a subsidiary low-Q cavity monitoring the beam phase, and using this information to damp phase oscillations.

The cooling system is of vital importance when using super-powered tubes, as their performance and life depend on a great deal of heat being removed from a small volume of copper. Also the water surrounds the grid insulator. This means that the water must be of very low conductivity, 0.2 microhms per cm. for the grid circuit and 1.0 microhms for all other circuits; and very well filtered. The flow and pressure requirements are quite high. Water is required for the 2054 and 2041 tubes and for the isolator and also for a waveguide water load. The cavities will be cooled by water tapped from the magnet supply, but in the Inner Hall the RF equipment will have its own water system employing 3 closed-circuit demineralised water circuits with heat exchangers to canal water. The highest purity circuit will have constant regeneration and filtering. The Inner Hall will be inhabitable during operation of the synchrotron, and the equipment will be manned by operators during commissioning. A minimum of operational controls and instrumentation will be taken to the main Control Room so that during normal routine operation of the machine it will not be necessary to man the local RF Controls.

## 6. VACUUM SYSTEM.

The main requirement for the vacuum system is a chamber which will enclose as much as possible of the magnet aperture and maintain a pressure in all parts lower than  $2 \times 10^{-6}$  torr. At this pressure only a few per cent of injected particles will be lost because of gas-scattering. The requirement is for an ultra-clean rather than an ultra-high vacuum system.

The chamber must be:—

- (i) Non-magnetic.
- (ii) Resistant to radiations.
- (iii) Manufactured in such a way as to prevent undue field distortions which could be produced from eddy currents.
- (iv) Able to withstand concentrated spot heating.

Test sections of different types of chamber have been made and from measurements on these, a composite titanium alloy and stainless steel structure, coated with glass reinforced epoxy resin will be used.

The total volume of the final system including RF cavities and pumping manifolds is about 4,500 litres.

The chamber itself is separated by isolation valves into 10 equal sectors of volume about 450 litres. Each of these sectors is pumped by four ion pumps of 125 litres/sec with an additional pump for each sector containing an RF cavity. These getter ion pumps were chosen for their ultra-clean performance and simplicity; a compact and commonly produced commercial type has a speed of 125 litres/sec.

The initial evacuation down to the starting pressure for the ion pumps is effected by a combination of rotary mechanical vane type pumps and high speed turbo-molecular pumps. This combination has a speed of 140 litres/sec from  $10^{-1}$ - $10^{-8}$  torr without refrigerated traps.

The mechanical pumps are started automatically in a sequence operated by pressure sensitive relays, and are automatically valved off and stopped when the ion pumps are working. In the event of a pressure rise the mechanical pump restarts automatically when the gas load on the ion pumps becomes too great.

Since the current in the pumps is directly proportional to pressure, the pumps themselves are used as pressure gauges. Some hot cathode gauges are available for checking purposes.

The ion pump currents are sampled cyclically and displayed on the data logger. Due to the low conduction of the vessel, a small leak shows as a peak on the display at the appropriate pump. This scan is automatic at a pre-set interval, or on demand by the operator.

Backing pressure measurement is by thermo-couple and Penning gauges.

All main controls are on a control centre in one of the D buildings with only the minimum of monitoring in the main control room. Some local control is also available.

## 7. INJECTION SYSTEM.

The injection system consists of a linear accelerator in which the electrons are accelerated to the required injection energy by the axial electric field associated with a RF wave travelling down an iris-loaded waveguide, together with the elements required for matching and deflecting the beam into the synchrotron.

As stated previously, the injection energy of 40 MeV has been settled by consideration of the minimum desirable magnetic field. The beam current of  $10 \mu\text{A}$  required from the synchrotron implies a circulating current of 272 mA, and in order to allow for the inflection period and the phase acceptance of the synchrotron, it will be necessary to inject a current of at least 440 mA. However, if it proves possible to modulate the electron beam from the injector at the synchrotron radio frequency, so that effectively all the current is concentrated into one bunch per cycle, the current required from the injector is 320 mA.

The linear accelerator has four sections of waveguide, each 2 m long. The RF power is supplied by two CSF klystrons, and each klystron feeds two sections. For the design beam current of 700 mA at 40 MeV, a peak power input of 10 MW into each section is required, and this is well within the maximum klystron rating of 30 MW. In order to ensure that at least 500 mA out of the total beam current comes within the close tolerance on energy ( $40 \pm 0.2$  MeV) and the low limit on emittance ( $3.2 \times 10^{-6}$  m. rad.), the electron beam from the triode gun is prebunched by velocity modulation, as in a klystron, before injection into the first section of waveguide, where the phase velocity of the RF wave is controlled to give optimum bunching of the electron beam and minimum energy spread.

At a later stage the electron beam injected into the accelerator will be modulated by chopping at 408 Mc/s to give one bunch per synchrotron cycle, while still maintaining an equivalent pulse current of 350 mA. The space charge forces produced by the large charge in each bunch are sufficient to modify the bunching mechanism, and this introduces problems which still have to be solved.

The electron beam from the injector is directed, by bending magnets, to intercept the equilibrium orbit at a small angle in one of the long straights. At this point, a pulsed electromagnetic inflector bends the beam onto the required orbit. Single turn injection is used, so that the inflector field must be constant for the time taken for an electron to make one revolution of the synchrotron, just under three quarters of a microsecond, and then fall to zero in as short a time as possible, to avoid deflecting the electrons out of the orbit. A number of quadrupole lenses in the injector path, together with the bending magnets, serve to match the emittance of the injector to the synchrotron acceptance, and to put electrons of differing momenta onto their correct closed orbits.

Provision has been made for the acceleration of positrons in the synchrotron. For this purpose, the electron injector will be used in connection with a positron conversion target. The electrons will strike a heavy metal target, producing bremsstrahlung. The absorption of the bremsstrahlung in a later part of the target will result in the production of electron-positron pairs. A proportion of these will be focused by a magnetic lens into a further section of the linear accelerator, phased so that the positrons are accelerated up to the required injection energy.



## APPENDIX

## PARAMETERS

## 1. MAGNET.

Magnetic radius of curvature ...	...	...	...	...	...	...	20.7697 m
Mean orbit radius ...	...	...	...	...	...	...	35.0937 m (115 ft 1.6 ins)
Orbital period ...	...	...	...	...	...	...	0.735 $\mu$ sec
Field at 4 GeV ...	...	...	...	...	...	...	6.43 kG
Field at injection energy 40 MeV ...	...	...	...	...	...	...	64.3 G
Focusing order ...	...	...	...	...	...	...	FODO
Number of magnets ...	...	...	...	...	...	...	40
Magnetic length of magnets ...	...	...	...	...	...	...	3.26250 m
Physical length of magnets ...	...	...	...	...	...	...	3.26250 m
Lengths of straight sections ...	...	...	...	...	...	...	alternately 3.5 m and 1 m
Number of betatron wavelengths per turn ...	...	...	...	...	...	...	5.25
Field index in F-Sector... ..	...	...	...	...	...	...	-46.169
Field index in D-Sector... ..	...	...	...	...	...	...	47.169
Field gradient in F ...	...	...	...	...	...	...	2.22% per cm
Field gradient in D ...	...	...	...	...	...	...	2.28% per cm
Maximum amplitude of betatron oscillation... ..	...	...	...	...	...	...	1.737 cm/m rad
Minimum amplitude of betatron oscillation ...	...	...	...	...	...	...	0.321 cm/m rad
Maximum closed orbit deviation for $\Delta p/p = 1\%$ ...	...	...	...	...	...	...	2.105 cm
Minimum closed orbit deviation for $\Delta p/p = 1\%$ ...	...	...	...	...	...	...	1.071 cm
Orbit compaction ( $\Delta r/r$ )/( $\Delta p/p$ ) ...	...	...	...	...	...	...	0.0453
Magnet gap in F-sector at equilibrium orbit... ..	...	...	...	...	...	...	2.4 ins
Magnet gap in D-sector at equilibrium orbit	...	...	...	...	...	...	3.0 ins
F-magnet horizontal aperture ...	...	...	...	...	...	...	5.12 ins
D-magnet horizontal aperture ...	...	...	...	...	...	...	3.54 ins
Lamination thickness ...	...	...	...	...	...	...	0.0185 ins
Weight of steel per F magnet ...	...	...	...	...	...	...	8.9 tons
Weight of steel per D magnet ...	...	...	...	...	...	...	9.2 tons
Total weight of magnet steel ...	...	...	...	...	...	...	362 tons
Beam height ...	...	...	...	...	...	...	5.0 ft

## 2. MAGNET COILS.

Number of coils per magnet ...	...	...	...	...	...	...	4
Number of turns per F magnet	...	...	...	...	...	...	32
Number of turns per D magnet	...	...	...	...	...	...	40
Cross-sectional area of copper conductor/turn	...	...	...	...	...	...	0.620 sq ins
Weight of copper conductor (F magnet)	...	...	...	...	...	...	0.895 tons
Weight of copper conductor (D magnet)	...	...	...	...	...	...	1.12 tons
Total weight of copper conductors	...	...	...	...	...	...	40.3 tons

## 3. MAGNET EXCITATION.

Nominal excitation frequency ...	...	...	...	...	...	...	50 cps
Peak air gap flux ...	...	...	...	...	...	...	9000 gauss
Inductance at peak field (F magnet) ...	...	...	...	...	...	...	0.02035 H
Inductance at peak field (D magnet) ...	...	...	...	...	...	...	0.02705 H
Peak stored energy in F magnet	...	...	...	...	...	...	18.8 kJ
Peak stored energy in D magnet	...	...	...	...	...	...	25.06 kJ
Total peak stored energy	...	...	...	...	...	...	877 kJ
rms AC voltage per F magnet	...	...	...	...	...	...	3.075 kV
rms AC voltage per D magnet	...	...	...	...	...	...	4.09 kV

Peak AC volts (to earth) per F magnet	...	...	...	...	...	4.34 kV
Peak AC volts (to earth) per D magnet	...	...	...	...	...	10.12 kV
Peak magnet current	...	...	...	...	...	1362 amps
rms magnet current	...	...	...	...	...	834 amps
DC component of magnet current	...	...	...	...	...	681 amps
AC component of magnet current (rms)	...	...	...	...	...	481 amps

#### 4. MAGNET POWER SUPPLY.

Number of sub-divisions of magnet network	...	...	...	...	...	10
In each sub-division:						
Number of series connected magnets	...	...	...	...	...	2 F, 2 D
Number of capacitor sections	...	...	...	...	...	1
Magnet inductance per sub-division	...	...	...	...	...	0.0948 Hy
Energy storage choke inductance per sub-division	...	...	...	...	...	0.1896 Hy
Resonant capacitance per sub-division (Magnet 107 $\mu$ F, Choke 53 $\mu$ F)	...	...	...	...	...	160 $\mu$ F
Capacitance/temperature coefficient ( $-10^\circ$ to $+35^\circ$ C)	...	...	...	...	...	0.01% per $^\circ$ C
rms AC voltage per sub-division	...	...	...	...	...	14.32 kV

##### (a) Resonant Capacitors.

Number of capacitor sections	...	...	...	...	...	10
Peak stored energy per capacitor section...	...	...	...	...	...	32.9 kJ
Total peak stored energy (excluding D.C. charge)	...	...	...	...	...	329 kJ
Total Reactive volt-amperes	...	...	...	...	...	103,000 kVAR

##### (b) Energy Storage Choke.

Number of secondary windings	...	...	...	...	...	10
Number of primary windings	...	...	...	...	...	10
Turns ratio ( $N_1 : N_2$ )	...	...	...	...	...	1 : 4
Inductance of each secondary at peak flux	...	...	...	...	...	0.1896 Hy
Peak energy stored in choke	...	...	...	...	...	987 kJ
rms AC secondary voltage...	...	...	...	...	...	14.32 kV
Peak secondary current	...	...	...	...	...	1021.5 amps
rms secondary current	...	...	...	...	...	722 amps
DC component of secondary current	...	...	...	...	...	681 amps
AC component of secondary current (rms)	...	...	...	...	...	241 amps

#### 5. RF PARAMETERS.

RF frequency	...	...	...	...	...	407.88 Mc/s
Subharmonic number of injector frequency	...	...	...	...	...	7
Orbital frequency	...	...	...	...	...	1.360 Mc/s
RF Harmonic Number	...	...	...	...	...	300
Number of accelerating cells	...	...	...	...	...	5 triple cavities
Free space wavelength	...	...	...	...	...	73.5 cm
Waveguide internal dimensions	...	...	...	...	...	$21 \times 10\frac{1}{2}$ ins
Waveguide over-all flange dimensions	...	...	...	...	...	$25\frac{1}{8} \times 14\frac{5}{8}$ ins
Guide wavelength	...	...	...	...	...	101.3 cm
Guide cut-off frequency	...	...	...	...	...	281 Mc/s
Number of sides to waveguide polygon	...	...	...	...	...	20
Radiation loss/turn at 4 GeV	...	...	...	...	...	1.10 MeV
Beam current	...	...	...	...	...	4            10 $\mu$ A
RF beam power at 4 GeV	...	...	...	...	...	120        300 kW
Total RF Power:						
Peak Power	...	...	...	...	...	480 kW
Average Power	...	...	...	...	...	150 kW

### 6. INJECTOR PARAMETERS.

Injection Energy	...	...	...	...	...	...	...	40 ± 0.2 MeV
Maximum beam emittance	...	...	...	...	...	...	...	$3.2 \times 10^{-6}$ m rad
Beam current within above limits	...	...	...	...	...	...	...	500 mA
Beam pulse length	...	...	...	...	...	...	...	1 μs
Radio frequency...	...	...	...	...	...	...	...	2855.17 Mc/s
Number of Sections of accelerator waveguide	...	...	...	...	...	...	...	4
Length of section	...	...	...	...	...	...	...	2 m
RF power input to each Section	...	...	...	...	...	...	...	10 MW
Number of klystrons	...	...	...	...	...	...	...	2
Rated power output per klystron	...	...	...	...	...	...	...	30 MW

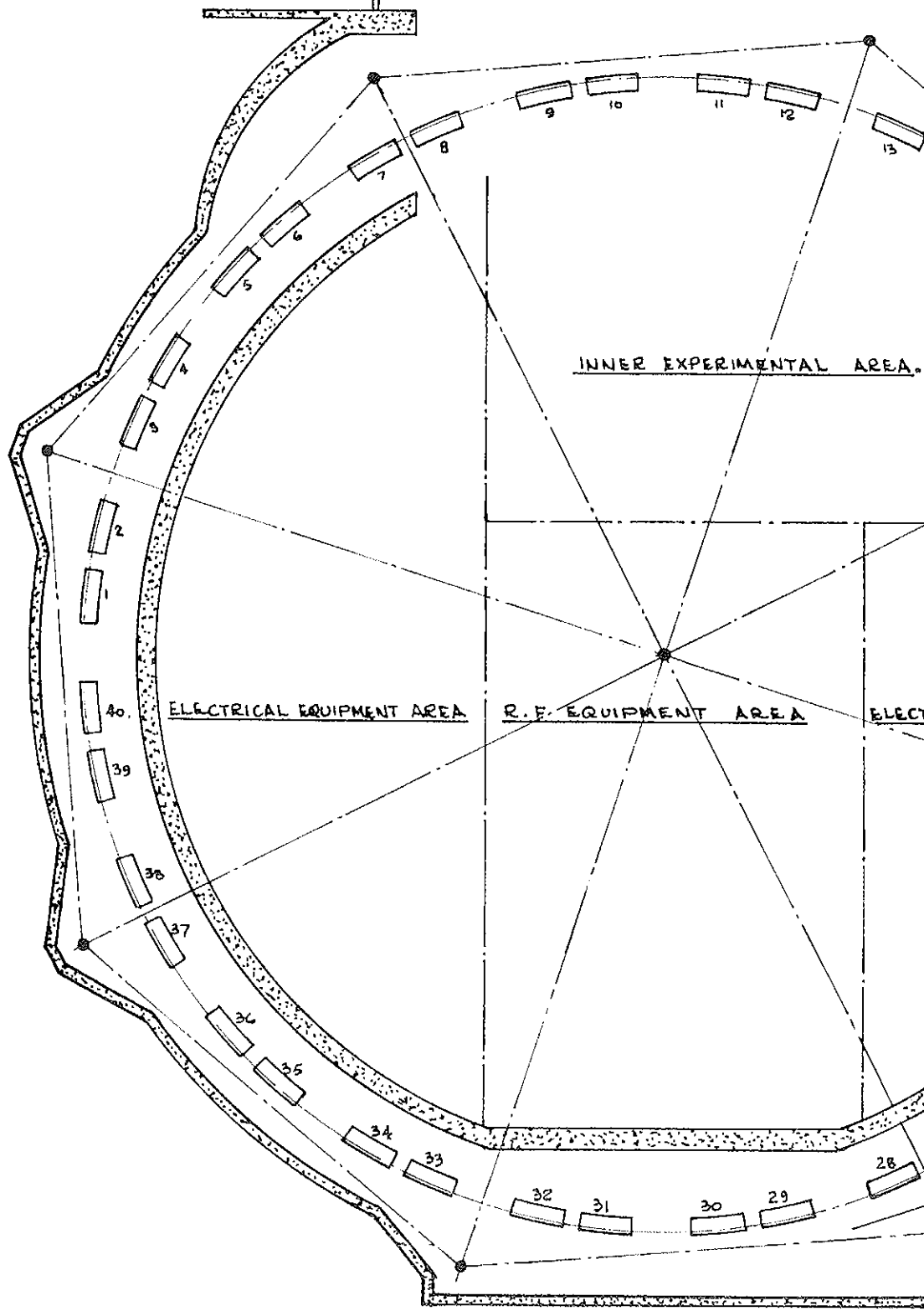
### 7. VACUUM SYSTEM.

Volume of vacuum system	...	...	...	...	...	...	...	4,500 litres
Number of ion pumps	...	...	...	...	...	...	...	51
Number of mechanical pumps...	...	...	...	...	...	...	...	10
Pumping speed of ion pumps	...	...	...	...	...	...	...	140 litres/sec
Pumping speed of mechanical pumps in range $10^{-2}$ torr to $10^{-7}$ torr	...	...	...	...	...	...	...	140 litres/sec
Conductance of half chamber length F magnet	...	...	...	...	...	...	...	28 litres/sec
D magnet	...	...	...	...	...	...	...	35 litres/sec





ELECTRON

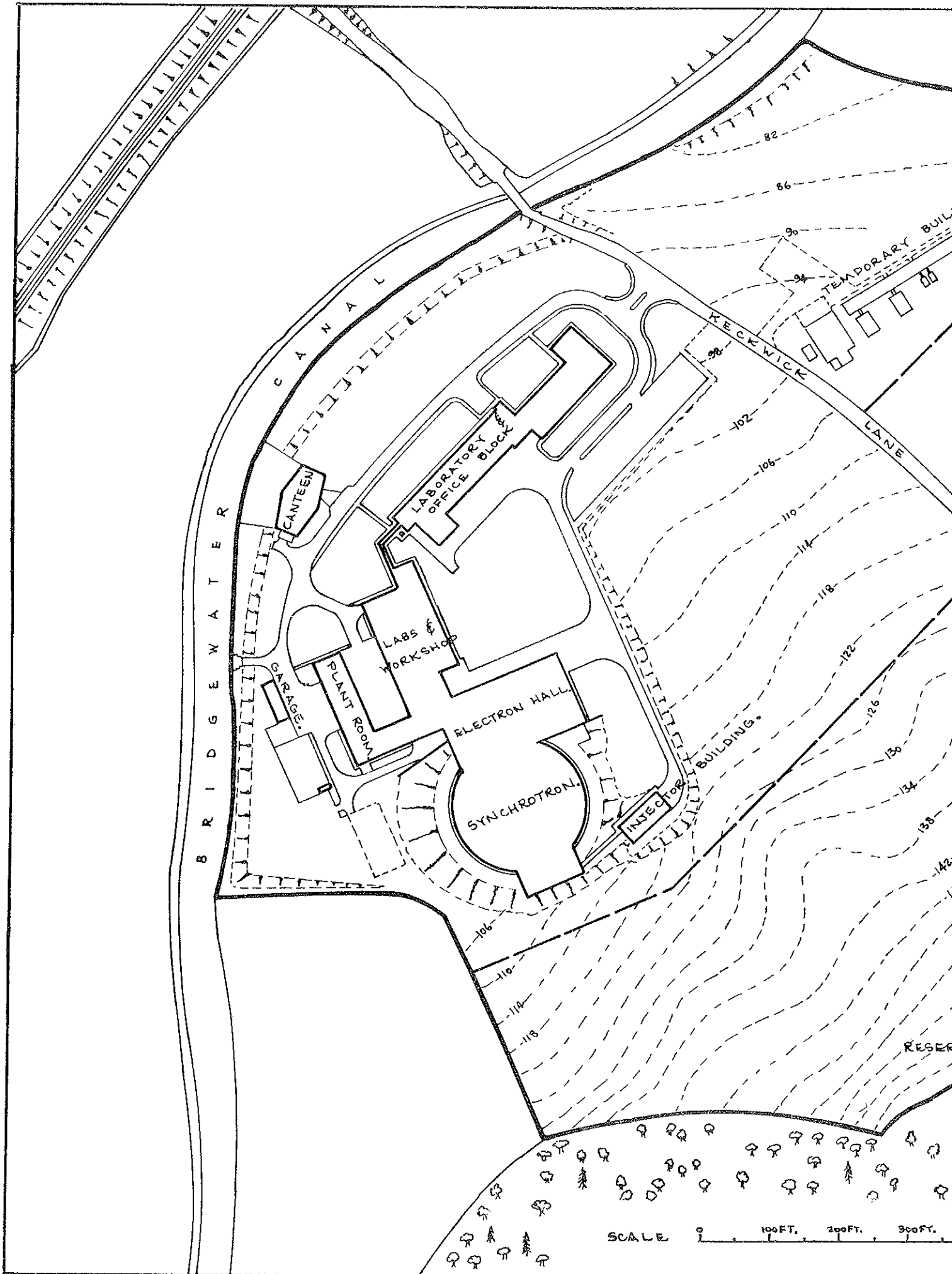


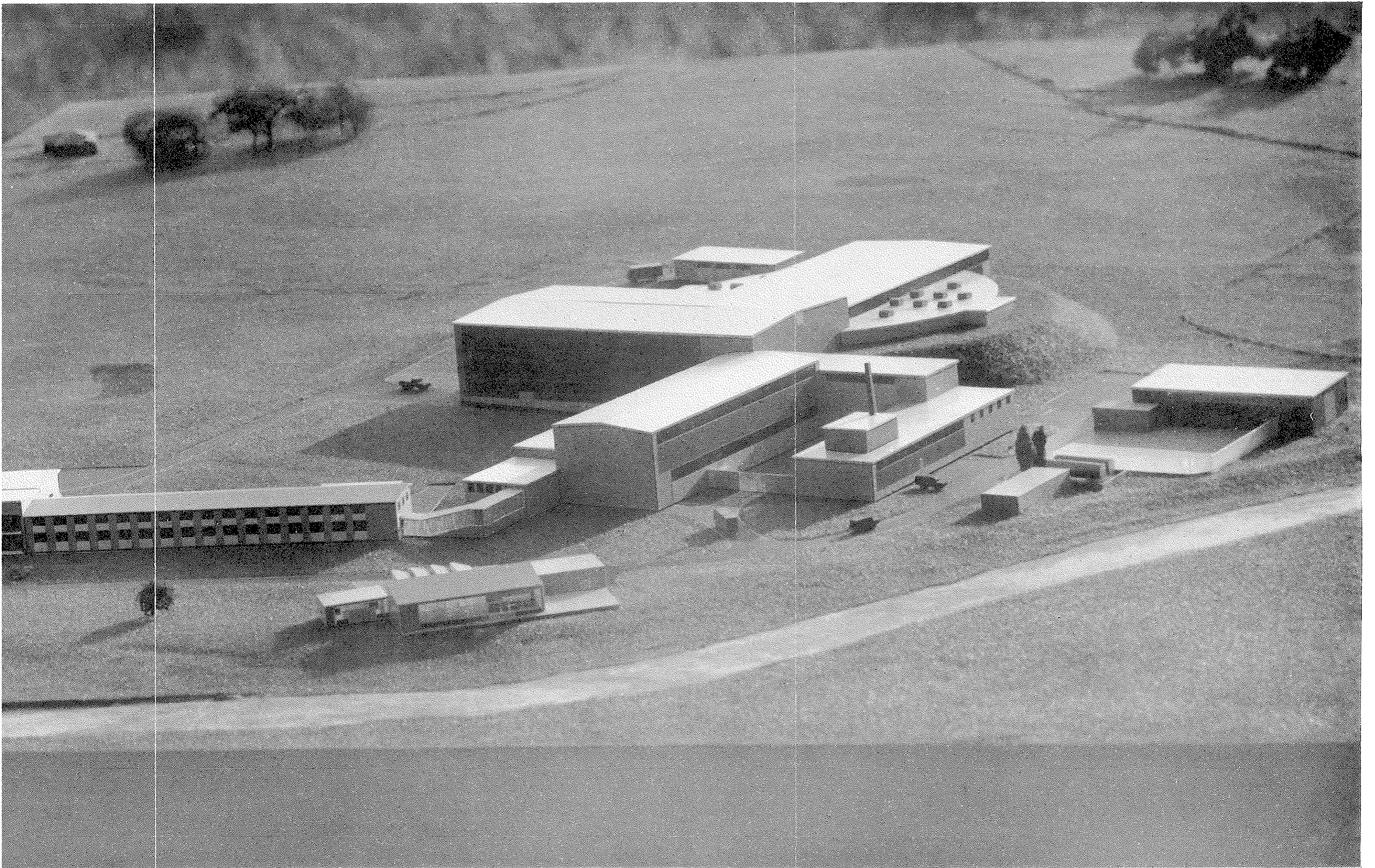
INNER EXPERIMENTAL AREA.

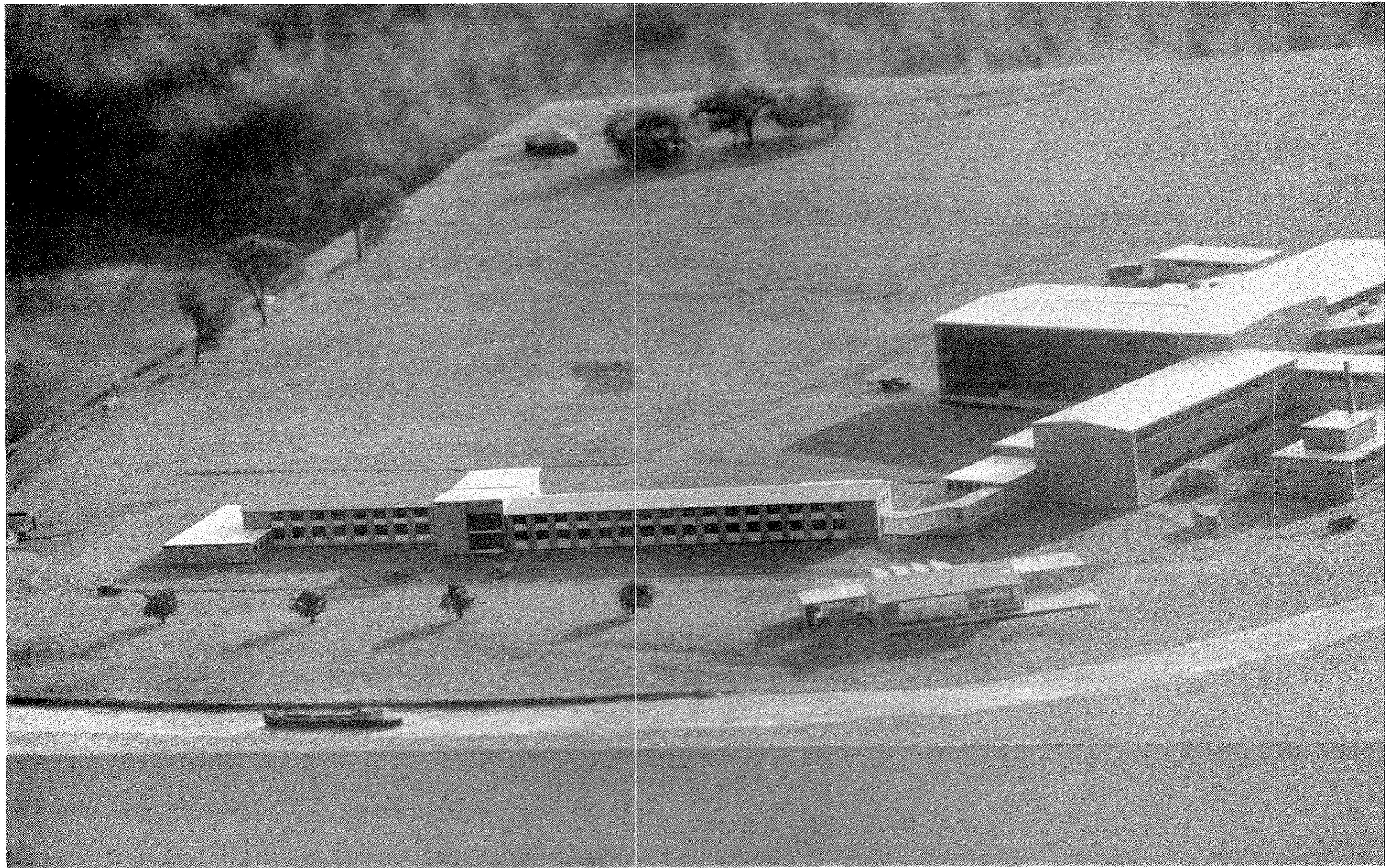
ELECTRICAL EQUIPMENT AREA

R.F. EQUIPMENT AREA

ELECT







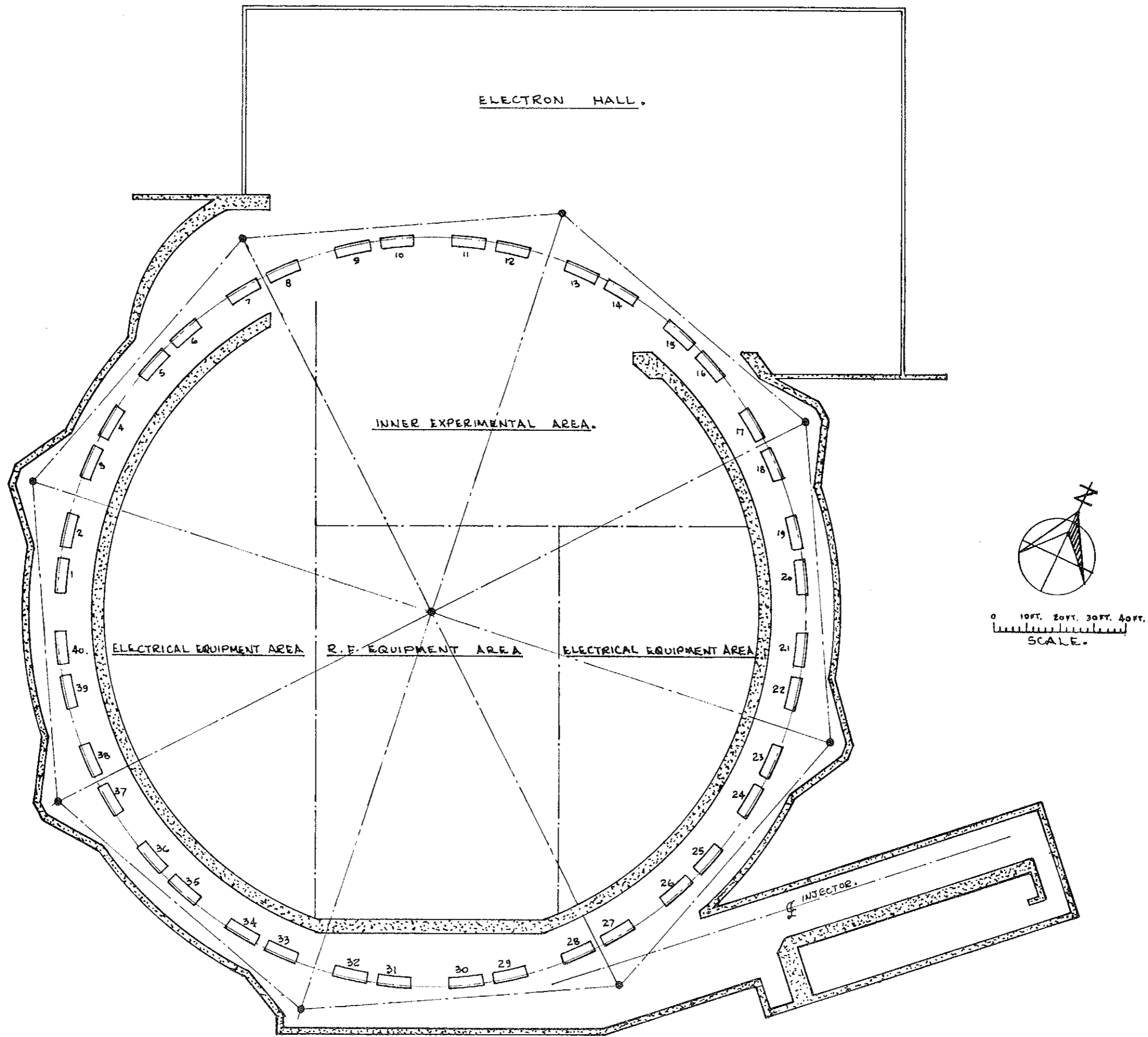


FIG. 1.

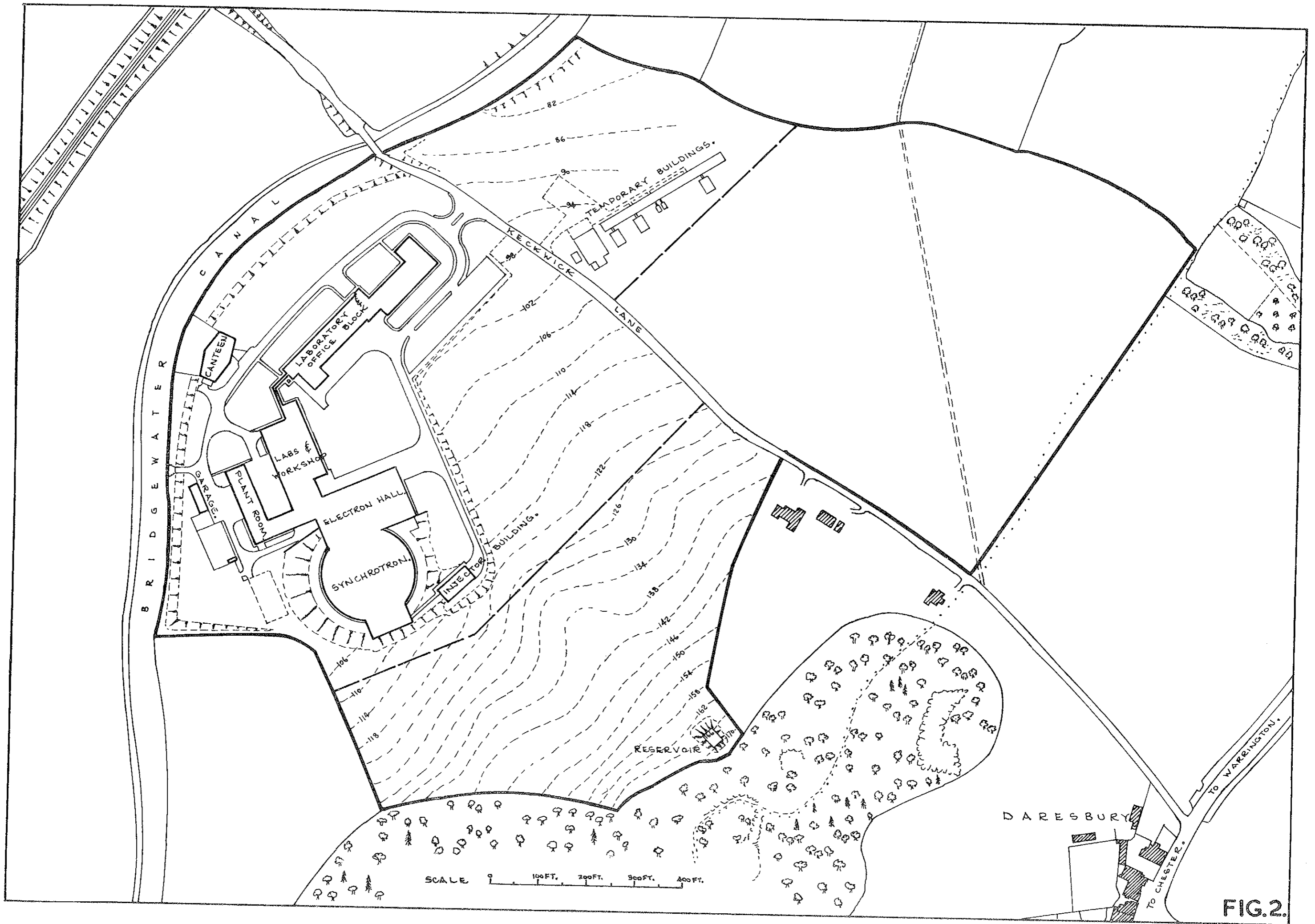
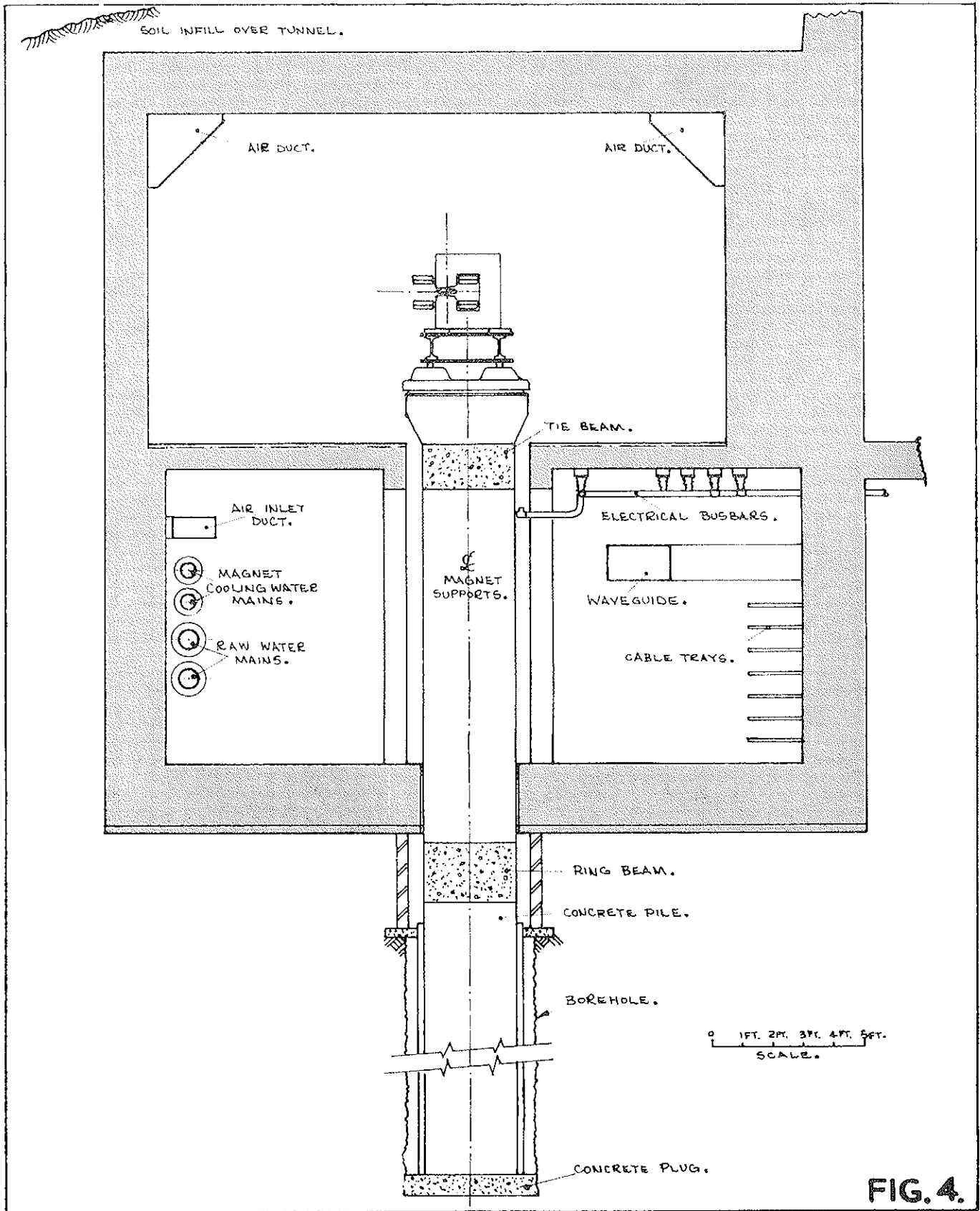
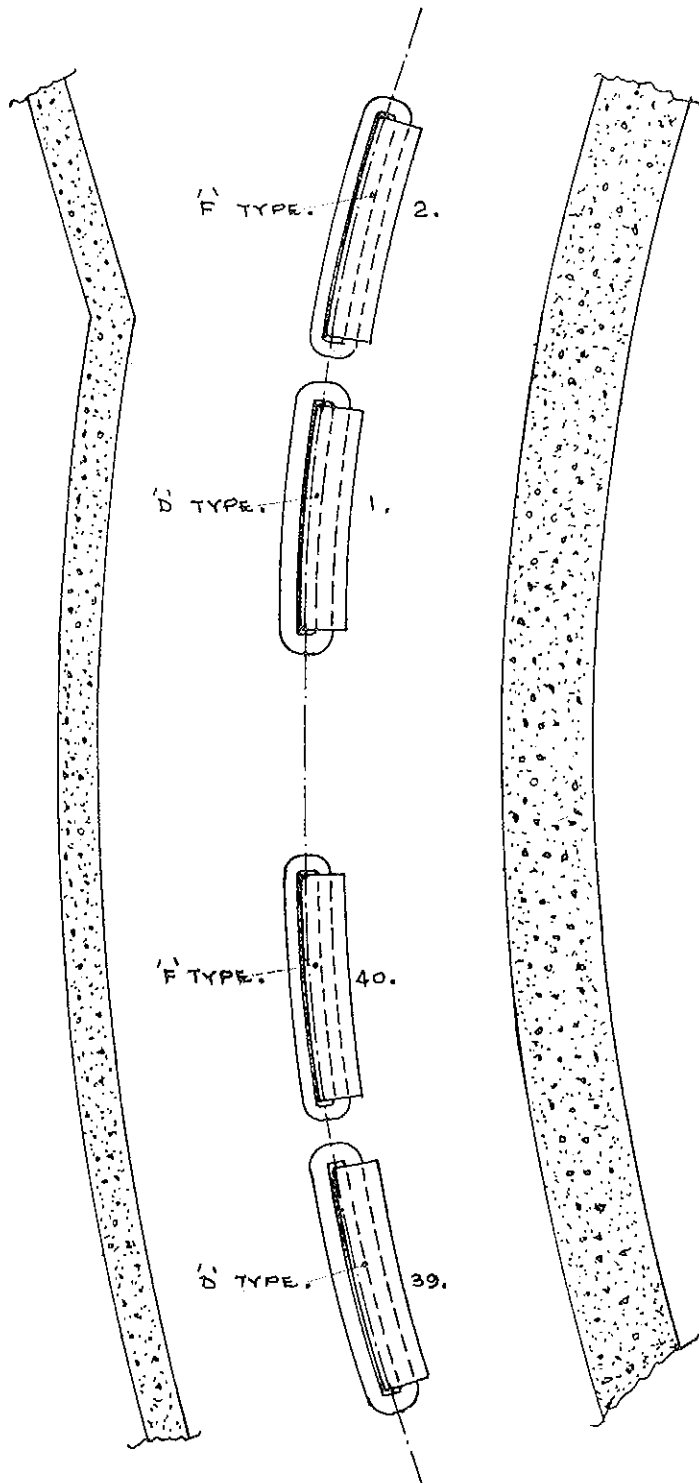


FIG. 2.

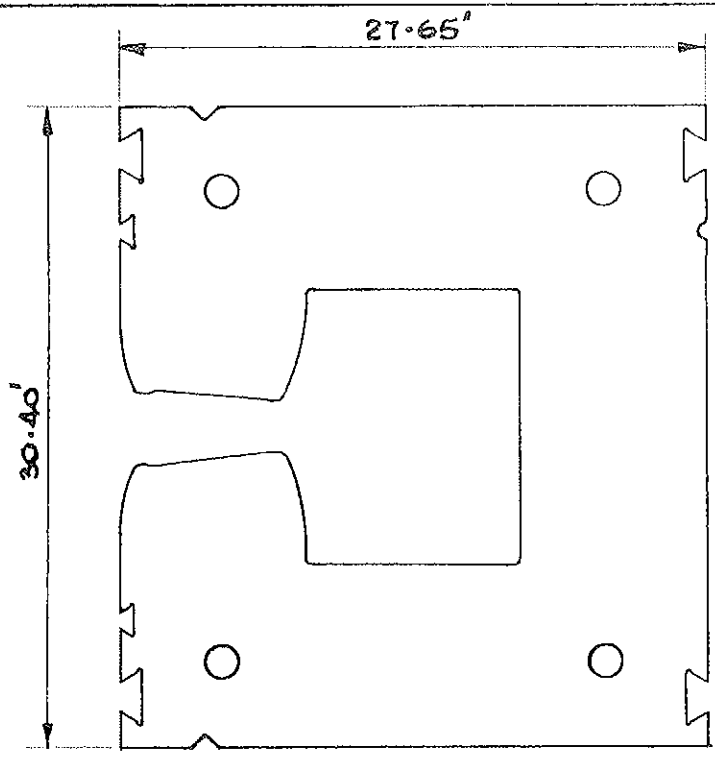




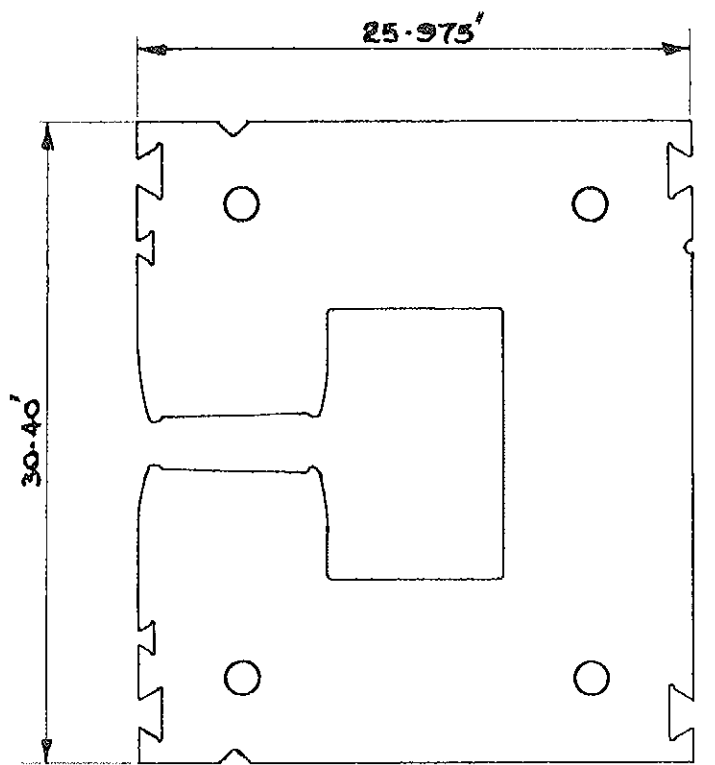


0 5 FT. 10 FT.  
SCALE.

FIG. 5.



D. TYPE MAGNET BLOCKS.



F. TYPE MAGNET BLOCKS

FIG. 6.

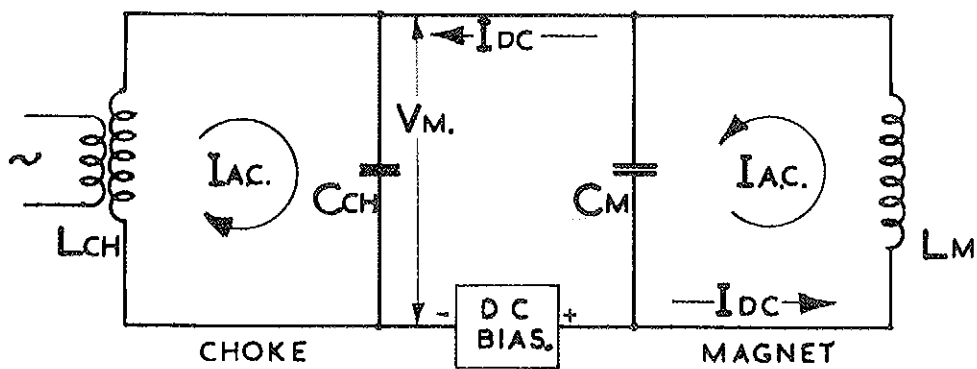


FIG. 7.

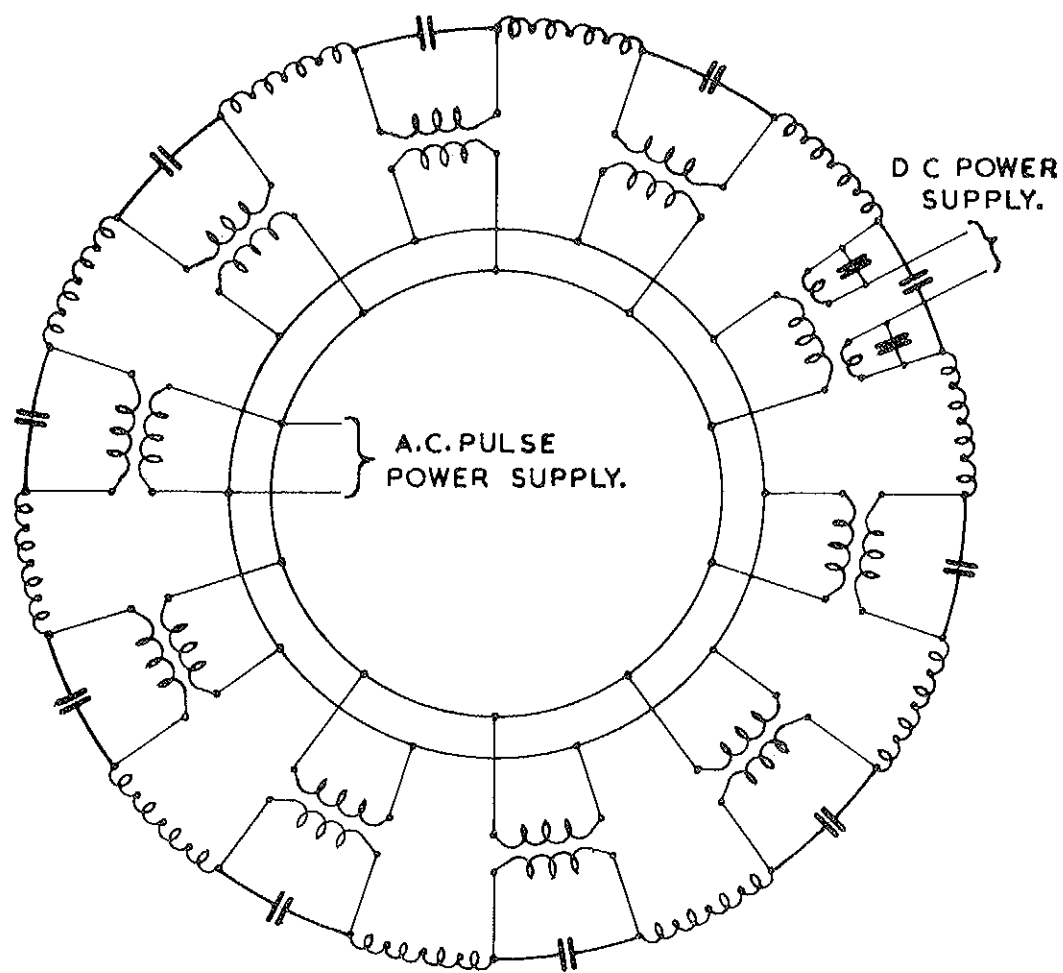


FIG. 8.